Mn-Containing Paramagnetic Conductors with Bis(ethylenedithio)tetrathiafulvalene (BEDT-TTF)

Samia Benmansour *, Yolanda Sánchez-Máñez and Carlos J. Gómez-García *

Instituto de Ciencia Molecular (ICMol), Universidad de Valencia, C/Catedrático José Beltrán 2, 46010 Valencia, Spain; yolsanma@gmail.com

* Correspondence: sam.ben@uv.es (S.B.); carlos.gomez@uv.es (C.J.G.-G.);
   Tel.: +34-9-6354-4423 (S.B. & C.J.G.-G.); Fax: +34-9-6354-3273 (S.B. & C.J.G.-G.)

Abstract: Two novel paramagnetic conductors have been prepared with the organic donor bis(ethylenedithio)tetrathiafulvalene (BEDT-TTF = ET) and paramagnetic Mn-containing metallic complexes: κ'-ET$_4$[KMn^{III}(C$_2$O$_4$)$_3$]·PhCN (**1**) and ET[Mn^{II}Cl$_4$]·H$_2$O (**2**). Compound **1** represents the first Mn-containing ET salt of the large Day's series of oxalato-based molecular conductors and superconductors formulated as (ET)$_4$[AM(C$_2$O$_4$)$_3$]·G (A^+ = H$_3$O$^+$, NH$_4^+$, K$^+$, ...; M^{III} = Fe, Cr, Al, Co, ...; G = PhCN, PhNO$_2$, PhF, PhCl, PhBr, ...). It crystallizes in the orthorhombic pseudo-κ phase where dimers of ET molecules are surrounded by six isolated ET molecules in the cationic layers. The anionic layers contain the well-known hexagonal honey-comb lattice with Mn(III) and H$_3$O$^+$ ions connected by C$_2$O$_4^{2-}$ anions. Compound **2** is one of the very few examples of ET salts containing ET^{2+}. It also presents alternating cationic-anionic layers although the ET molecules lie parallel to the layers instead of the typical almost perpendicular orientation. Both salts are semiconductors with room temperature conductivities of ca. 2×10^{-5} and 8×10^{-5} S/cm and activation energies of 180 and 210 meV, respectively. The magnetic properties are dominated by the paramagnetic contributions of the high spin Mn(III) ($S = 2$) and Mn(II) ($S = 5/2$) ions.

Keywords: electro-crystallization; ET-salts; paramagnetic conductors; electrical conductivity; magnetic properties; Mn(II) complexes; Mn(III) complexes

1. Introduction

The design and synthesis of multifunctional molecular materials combining electrical and magnetic properties is one of the main challenges in the field of molecular materials [1–4]. An advantage of these materials is that they offer the possibility to study the competition and interplay of these two properties. So far, a large number of molecular materials combining magnetism with conductivity has been obtained. These examples include superconductors with paramagnetic complexes [1,5–9] or with antiferromagnetic lattices [10–15] and ferromagnetic conductors [4,16].

Among the different paramagnetic complexes used to prepare these materials, tris(oxalato)metalate complexes, [M(C$_2$O$_4$)$_3$]$^{n-}$, are, by far, the most used ones. These anions may crystallize as:

(i)   Monomers as in (TTF)$_7$[Fe(C$_2$O$_4$)$_3$]$_2$·4H$_2$O [17], (TTF)$_3$[Ru(C$_2$O$_4$)$_3$]·(EtOH)$_{0.5}$·4H$_2$O [18], (BEST)$_4$[M(C$_2$O$_4$)$_3$]·PhCOOH·H$_2$O [19], (BEST)$_4$[M(C$_2$O$_4$)$_3$]·1.5H$_2$O [19], (M = Cr and Fe), (BEST)$_9$[Fe(C$_2$O$_4$)$_3$]$_2$·7H$_2$O [19], (ET)$_2$[Ge(C$_2$O$_4$)$_3$]·PhCN [20], (ET)$_9$Na$_{18}$[M(C$_2$O$_4$)$_3$]$_8$·24H$_2$O (M^{III} = Fe and Cr) [21,22], (ET)$_{12}$[Fe(C$_2$O$_4$)$_3$]$_2$·nH$_2$O [23], (ET)$_5$[Fe(C$_2$O$_4$)$_3$]·CH$_2$Cl$_2$·2H$_2$O [24], (ET)$_5$[Ge(C$_2$O$_4$)$_3$]$_2$ [25] and (ET)$_7$[Ge(C$_2$O$_4$)$_3$](CH$_2$Cl$_2$)$_{0.87}$(H$_2$O)$_{0.09}$ [25]. (TTF = tetrathiafulvalene; BEST = bis(ethylenediseleno)-tetrathiafulvalene; ET = bis(ethylenedithio)tetrathiafulvalene).

(ii) Previously unknown $[M_2(C_2O_4)_5]^{4-}$ dimers (M^{III} = Fe and Cr) with TTF, TMTTF (tetramethyl-tetrathiafulvalene) and ET [17,26].

(iii) Previously unknown $[\{M^{III}(C_2O_4)_3\}_2M^{II}(H_2O)_2]^{4-}$ trimers (M^{III} = Cr and Fe; M^{II} = Mn, Fe, Co, Ni, Cu and Zn) only obtained with TTF [27,28].

(iv) Forming honeycomb-like 2D anionic layers as in the first molecular ferromagnetic metals: $(ET)_3[Mn^{II}Cr^{III}(C_2O_4)_3]$ and $(BETS)_x[Mn^{II}Cr^{III}(C_2O_4)_3]\cdot CH_2Cl_2$ (BETS = bis(ethylenedithio) tetraselenafulvalene; $x \approx 3$) [4,16,29–31], and also in the Day's series of paramagnetic superconductors, metals and semiconductors formulated as $(ET)_4[A^IM^{III}(C_2O_4)_3]\cdot G$ (A^I = H_3O^+, K^+ and NH_4^+; M^{III} = Cr, Fe, Ga, Co, Mn and Al; G = PhCN, PhNO$_2$, py, PhCl$_2$, PhF, PhCl, PhBr, PhCOCH$_3$, PhCH$_2$OHCH$_3$, Me$_2$NCHO, CH$_2$Cl$_2$, PhN(CH$_3$)CHO, PhCH$_2$CN, . . .) [1]. This series constitutes, by far, the largest family of paramagnetic superconductors, metals and semiconductors prepared to date. In this series, we can distinguish three different crystal structures: (i) a $C2/c$ (#15) monoclinic β'' phase (Table 1); (ii) an orthorhombic $Pbcn$ (#60) pseudo-κ phase (Table 2) and (iii) a triclinic $P1$ (#1) or P-1 (#2) $\alpha\beta''$ or α-pseudo-κ phase (Table 3). Besides these three 4:1 series, there is a fourth series with 3:1 cation:anion stoichiometry with either triclinic $P1$ (#1), monoclinic $P2_1$ (#4) and $P2_1/c$ (#14) or orthorhombic $P2_12_12_1$ (#19) crystal structures (Table 4). The main difference between these four series lies in the disposition of the organic molecules in the cationic layers. The monoclinic $C2/c$ (#15) β'' phase presents parallel ET molecules, the orthorhombic $Pbcn$ (#60) pseudo-κ phase contains ET dimers surrounded by six monomers, the triclinic phase presents a mixture of alternating θ and β'' (or θ and pseudo-κ) layers, and, finally, the 3:1 salts present alternating tilted dimers and monomers. These structural differences lead to different physical properties: the triclinic and orthorhombic phases are semiconductors (Tables 2–4), whereas the monoclinic salts are metallic or even superconductors (Table 1).

Table 1. Structural and electrical properties of the monoclinic $(ET)_4[A^IM^{III}(C_2O_4)_3]\cdot G$ salts.

CCDC Code	M^{III}	A^I	G	Packing	SG	Elect. Prop.	Ref.
ZIGYET	Fe	H_3O^+	PhCN	β''	$C2/c$	T_c = 7.0–8.5 K	[6,7,32–34]
KILFOB/GOC/GUI/HAP	Fe	H_3O^+	$C_5H_5N_{(1-x)}$/PhCN$_x$	β''	$C2/c$	T_c = F(x)	[33]
BEMPEO/QAL	Fe	H_3O^+	C_5H_5N	β''	$C2/c$	T_{MI} = 116 K	[33,35]
ECOPIV	Fe	H_3O^+/NH_4^+	PhNO$_2$	β''	$C2/c$	T_c = 6.2 K	[36]
COQNEB	Fe	H_3O^+	PhNO$_2$	β''	$C2/c$	Semicond	[37,38]
PONMEL	Fe	H_3O^+	PhCl$_2$	β''	$C2/c$	T_{MI} = 3.0 K, Metal > 1.5 K	[34,39]
SAPWEM	Fe	H_3O^+	PhBr	β''	$C2/c$	T_c = 4.0 K	[40]
UMACEQ	Fe	NH_4^+	DMF	β''	$C2/c$	Metal > 4 K	[41]
UJOXEX	Fe	H_3O^+	PhF	β''	$C2/c$	T_c = 1.0 K	[34,42,43]
UJOXAT	Fe	H_3O^+	PhCl	β''	$C2/c$	Metal > 0.4 K	[34,42–45]
UJOXIB	Fe	H_3O^+	PhF/PhCN	β''	$C2/c$	T_c = 6.0 K	[34,42]
UJOXOH	Fe	H_3O^+	PhCl$_2$/PhCN	β''	$C2/c$	T_c = 7.2 K	[34]
UJOYAU	Fe	H_3O^+	PhCl/PhCN	β''	$C2/c$	T_c = 6.0 K	[34,42]
UJOYEY	Fe	H_3O^+	PhBr/PhCN	β''	$C2/c$	T_c = 4.2 K	[34,42]
QAXSIT	Fe	K^+	PhI	β''	$C2/c$	E_a = 64 meV	[43]
-	Fe	K^+	PhCl	β''	-	Semicond.	[46]
-	Fe	Rb^+	C_5H_5N	β''	-	Metal > 4.2 K	[44]
JUPGUW01	Cr	H_3O^+	PhCN	β''	$C2/c$	T_c = 5.5–6.0 K	[32,47]
MEQZIR	Cr	H_3O^+	CH$_2$Cl$_2$	β''	$C2/c$	T_{MI} = 150 K	[48]
ECOPUH	Cr	H_3O^+/NH_4^+	PhNO$_2$	β''	$C2/c$	T_c = 5.8 K	[36]
-	Cr	H_3O^+	PhBr	β''	$C2/c$	T_c = 1.5 K	[45]
-	Cr	H_3O^+	PhCl	β''	$C2/c$	T_{MI} = 130 K	[45]
UMACAM	Cr	K^+/NH_4^+	DMF	β''	$C2/c$	Metal > 4 K	[41]
UMACIU	Cr	K^+	DMF	β''	$C2/c$	Metal > 4 K	[41]
HUNQIQ	Ga	H_3O^+	C_5H_5N	β''	$C2/c$	$T_c \approx 2$ K	[49]
HUNQUC	Ga	H_3O^+	PhNO$_2$	β''	$C2/c$	T_c = 7.5 K	[49]
HOBROH	Ga	H_3O^+/K^+	PhBr	β''	$C2/c$	metal > 0.5 K	[50]
UDETUU	Ru	H_3O^+/K^+	PhCN	β''	$C2/c$	T_c = 6.3 K	[51]
YUYTUJ	Fe	H_3O^+	2-Cl–Py	β''	$C2/c$	T_c = 4.0 K	[52]
YUYVEV	Fe	H_3O^+	2-Br–py	β''	$C2/c$	T_c = 4.3 K	[52]
YUYVOF	Fe	H_3O^+	3-Cl–py	β''	$C2/c$	metal > 0.5 K	[52]
YUYVUL	Fe	H_3O^+	3-Br–py	β''	$C2/c$	metal > 0.5 K	[52]
DUDWOQ	Fe	Li^+ + H_2O	EtOH	η (α'')	$P2_1/n$	E_a = 80 meV	[53]
-	Mn	H_3O^+	PhBr	β''	$C2/c$	T_c = 2.0 K	[43]

T_c = superconducting temperature; T_{MI} = metal insulator temperature; E_a = activation energy.

Table 2. Structural and electrical properties of the orthorhombic $(ET)_4[A^IM^{III}(C_2O_4)_3]\cdot G$ salts.

CCDC Code	M^{III}	A^I	G	ET Packing	Space Group	Electrical Properties	Ref.
UJOXUN	Fe	H_3O^+	PhF/PhCN	pseudo-κ	*Pbcn*	Semiconductor	[34]
ZIWNEY	Fe	NH_4^+	PhCN	pseudo-κ	*Pbcn*	E_a = 140 meV	[7,32]
ZIWNIC	Fe	K^+	PhCN	pseudo-κ	*Pbcn*	E_a = 141 meV	[7]
JUPGUW	Cr	H_3O^+	PhCN	pseudo-κ	*Pbcn*	E_a = 153 meV	[32,47]
QIWMOY	Co	NH_4^+	PhCN	pseudo-κ	*Pbcn*	E_a = 225 meV	[32]
QIWMUE	Al	NH_4^+	PhCN	pseudo-κ	*Pbcn*	E_a = 222 meV	[32]
UDETOO	Ru	H_3O^+/K^+	PhCN	pseudo-κ	*Pbcn*	-	[51]
1	Mn	K^+	PhCN	pseudo-κ	*Pbcn*	E_a = 180 meV	this work

E_a = activation energy.

Table 3. Structural and electrical properties of the triclinic $(ET)_4[A^IM^{III}(C_2O_4)_3]\cdot G$ salts.

CCDC Code	M^{III}	A^I	G	ET Packing	Space Group	Electrical Properties	Ref.
TANDIX	Fe	H_3O^+	PhBr$_2$	α + κ	*P*-1	Metal > 0.4 K	[34,54]
HOBRIB	Ga	H_3O^+/K^+	PhBr$_2$	α + κ	*P*-1	metal > 0.5 K	[50]
ARABEA	Fe	NH_4^+	PhCOCH$_3$	α + β″	*P*-1	No supercond	[55]
CILDIL	Fe	NH_4^+	R/S-Ph-CH$_2$OHCH$_3$	α + β″	*P*-1	T_{MI} = 170 K	[56]
NIPTEM	Fe	NH_4^+	S-PhCH$_2$OHCH$_3$	α + β″	*P*-1	T_{MI} = 150 K	[56]
AQUZUH	Ga	NH_4^+	PhN(Me)CHO	α + β″	*P*-1	Semicond	[55]
ARABAW	Ga	NH_4^+	PhCH$_2$CN	α + β″	*P*-1	Semicond	[55]

T_{MI} = metal insulator temperature.

Table 4. Structural and electrical properties of $(ET)_3[A^IM^{III}(C_2O_4)_3]\cdot G$ salts.

CCDC Code	M^{III}	A^I	G	ET Packing	Space Group	Electrical Properties	Ref.
BOYTIU	Al	Na^+	CH_3NO_2	dimers + mon.	$P2_1$	E_a ≈ 140 meV	[57]
XUNXOU01	Cr	Na^+	CH_3NO_2	dimers + mon.	$P2_1$	E_a = 79 meV	[58]
XUNXOU	Cr	Na^+	CH_3NO_2	dimers + mon.	$P2_12_12_1$	E_a = 80 meV	[58]
-	Cr	NH_4^+	CH_3NO_2	dimers + mon.	$P2_12_12_1$	E_a = 80 meV	[58]
DUXNOA	Cr	Na^+	CH_2Cl_2	dimers + mon.	*P*1	E_a = 69 meV	[22]
DUDWUW	Cr	Li^+	EtOH	dimers + mon.	$P2_1/c$	E_a = 179 meV	[53]
-	Fe	Li^+	EtOH	dimers + mon.	$P2_1/c$	E_a = 126 meV	[53]
KOGMUG01	Cr	Na^+	CH_3CN	dimers + mon.	$P2_1$	E_a = 79 meV	[59]
-	Cr	Na^+	DMF	θ-packing	*P*1	E_a = 43 meV	[59]
YUCLOZ	Cr	Na^+	EtOH	dimers + mon.	*P*1	no data	[59]

One of the advantages of these series of compounds is the possibility to tune the electrical properties by simply changing the guest solvent molecule (*G*) located in the centre of the hexagonal cavities formed by the anionic lattice. This guest molecule may interact with the ET molecules, promoting the ordering of the ethylene groups of the ET molecules and, thus, stabilizing the superconductor state [60] as in the case of *G* = PhCN and PhNO$_2$ [6,7,36,49,61] whose radical salts are superconductors and present the highest T_c's in these series: (T_c = 6.0, 8.5, 5.8, 6.2 and 7.5 K for *G*/*M* = PhCN/Cr and PhCN/Fe, PhNO$_2$/Cr, PhNO$_2$/Fe and PhNO$_2$/Ga, respectively, Table 1). For *G* = pyridine [35,49], dichloromethane [48] or dimethylformamide [41], the disorder remains down to very low temperatures and the salts are not superconductors or present very low T_c. Even more, the mixture of PhCN with other solvents as C_5H_5N, PhCl$_2$, PhNO$_2$, PhF, PhCl or PhBr changes the ordering effect of the solvent and allows a fine tuning of T_c [33,34].

Although many different guest molecules have been used (see Tables 1–4), the number of trivalent metals used to date is quite limited. Thus, most of the reported salts contain Fe (30 salts), Cr (16 salts) or Ga (6 salts). There are also two reported examples with Ru, two with Al and one with Co. Surprisingly,

no radical salts with other trivalent metal ions have been reported to date. In order to investigate the effect of other trivalent metal ions on the final structure and on the physical properties, we have used the $[Mn(C_2O_4)_3]^{3-}$ anion with ET under different synthetic conditions. Here, we present the synthesis, structure, magnetic and electrical properties of the first example of radical salt of the Day's series obtained with Mn(III): κ'-(ET)$_4$[KMn^{III}(C$_2$O$_4$)$_3$]·PhCN (**1**) and of a very original salt obtained with the same $[Mn(C_2O_4)_3]^{3-}$ anion but using different synthetic conditions: (ET)[MnCl$_4$]·H$_2$O (**2**).

2. Results and Discussion

2.1. Syntheses of the Complexes

The synthesis of the two radical salts was performed using the same precursor K$_3$[Mn(C$_2$O$_4$)$_3$] salt (and 18-crown-6 in order to solubilize this salt, see the Experimental section). The main difference is the use of different solvents: a 10:1 (*v/v*) mixture of PhCN and MeOH for compound **1** and a 10:1 (*v/v*) mixture of 1,1,2-trichloroethane (TCE) and MeOH for **2**. An additional difference is the use of benzoic acid in the synthesis of compound **1**. Interestingly, benzoic acid does not enter in the structure, but it seems to facilitate the crystallization of the final salt. In fact, attempts to obtain compound **1** without the use of benzoic acid failed. In summary, the use of PhCN gives rise to compound (ET)$_4$[KMn^{III}(C$_2$O$_4$)$_3$]·PhCN (**1**), whereas TCE results in a totally different compound (ET)[MnCl$_4$]·H$_2$O (**2**) with ET^{2+} instead of ET$^{+0.5}$ and with $[Mn^{II}Cl_4]^{2-}$ instead of $[Mn^{III}(C_2O_4)_3]^{3-}$. The question is straightforward: why is the solvent so important in the final product? The answer seems to be related with the much lower solubility of the precursor K$_3$[Mn(C$_2$O$_4$)$_3$] in TCE. This lower solubility increases the resistance of the electrochemical cell since the concentration of anions is lower. The higher resistance increases the potential of the source needed to apply the desired constant intensity since the electrochemical synthesis is performed under constant current. The higher voltage results in the cathode in the oxidation of ET to ET^{2+} and in the anode in the reduction of Mn(III) to Mn(II). Additionally, the intensity and time used for compound **2** were higher than for **1** (see experimental section). Finally, the partial decomposition of TCE liberates chloride anions that coordinate to Mn(II) to form the observed $[MnCl_4]^{2-}$ anion. Note that the release of chloride anions from the decomposition of chlorinated solvents is quite common in the synthetic conditions of the electrochemical cells and has been observed in other ET salts [62–64].

2.2. Description of the Structures

Structure of (ET)$_4$[KMn^{III}(C$_2$O$_4$)$_3$]·PhCN (**1**). Compound **1** crystallizes in the orthorhombic space group *Pbcn* (Table 5) and is isostructural to those obtained with other trivalent metal ions as Fe, Cr, Co and Al and different monovalent cations as H$_3$O$^+$, NH$_4^+$ and K$^+$ (Table 2). Interestingly, there is only one reported example with K$^+$ as monovalent cation and there is no example with Mn(III) as a trivalent cation.

The asymmetric unit contains two independent ET molecules (labelled as A and B) lying on general positions, half $[Mn(C_2O_4)_3]^{3-}$ anion, half benzonitrile molecule and half K$^+$ cation, all lying on a two-fold rotation axis. Figure 1 shows the ellipsoid diagram of the molecules in **1** together with the atom-labelling scheme.

The crystal structure consists of alternating layers of ET molecules adopting the pseudo-κ phase and anionic layers containing $[Mn(C_2O_4)_3]^{3-}$ anions, K$^+$ cations and the guest benzonitrile molecule (Figure 2).
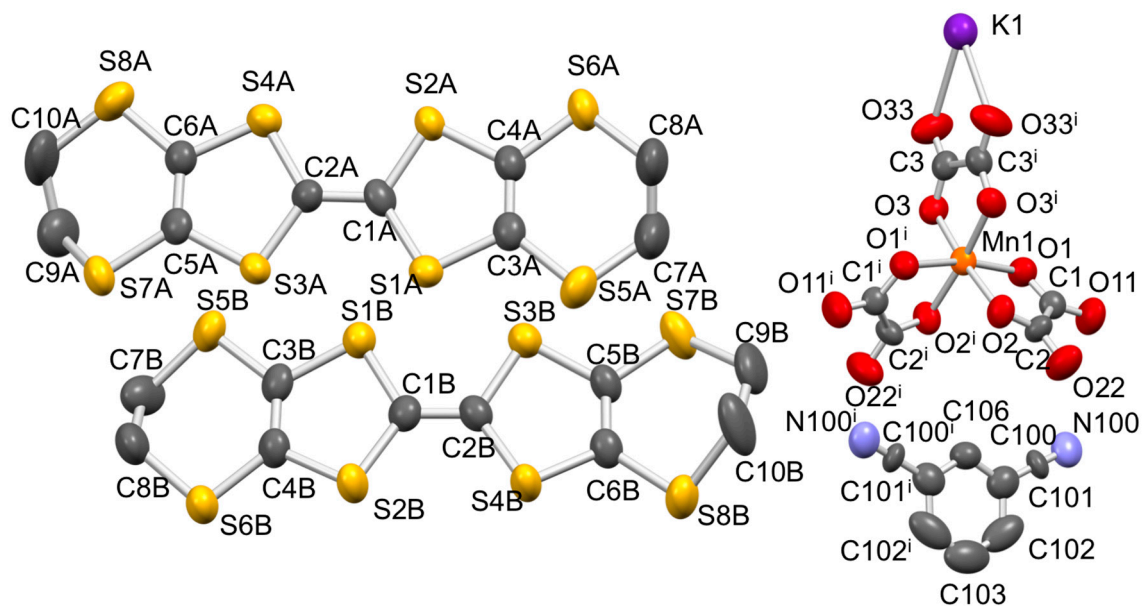
Figure 1. Thermal ellipsoid diagram (at 50% probability) of the molecules in compound **1**. Symmetry code: i = $-x, y, 1/2-z$.

Table 5. Crystal data and structure refinement of compounds **1** and **2**.

Compound	1	2
Formula	$C_{53}H_{36}KMnNO_{12}S_{32}$	$C_{10}H_{10}MnCl_4OS_8$
F. Wt.	1999.97	599.45
Space group	*Pbcn*	*Pnna*
Crystal system	Orthorhombic	Orthorhombic
a (Å)	10.3727 (4)	12.3724 (9)
b (Å)	19.6588 (8)	12.3738 (9)
c (Å)	36.2145 (13)	13.7726 (13)
$V/\text{Å}^3$	7384.7 (5)	2108.5 (3)
Z	4	4
T (K)	120	120
$\rho_{calc}/\text{g·cm}^{-3}$	1.798	1.856
μ/mm^{-1}	1.199	1.923
$F(000)$	4052	1156
R(int)	0.1380	0.1089
θ range (deg)	2.910–25.053	2.958–25.044
Total reflections	59,518	14,081
Unique reflections	6534	1867
Data with $I > 2\sigma$ (I)	6534	1867
N_{var}	462	114
R_1 [a] on $I > 2\sigma$ (I)	0.0700	0.0509
wR_2 [b] (all)	0.1729	0.1006
GOF [c] on F^2	1.011	1.080
$\Delta\rho_{max}$ (eÅ^{-3})	0.561	1.130
$\Delta\rho_{min}$ (eÅ^{-3})	−0.839	−0.553

[a] $R_1 = \Sigma||F_o| - |F_c||/\Sigma|F_o|$. [b] $wR_2 = [\Sigma w(F_o^2 - F_c^2)^2/\Sigma w(F_o^2)^2]^{1/2}$. [c] GOF $= [\Sigma[w(F_o^2 - F_c^2)^2/(N_{obs} - N_{var})]^{1/2}$.
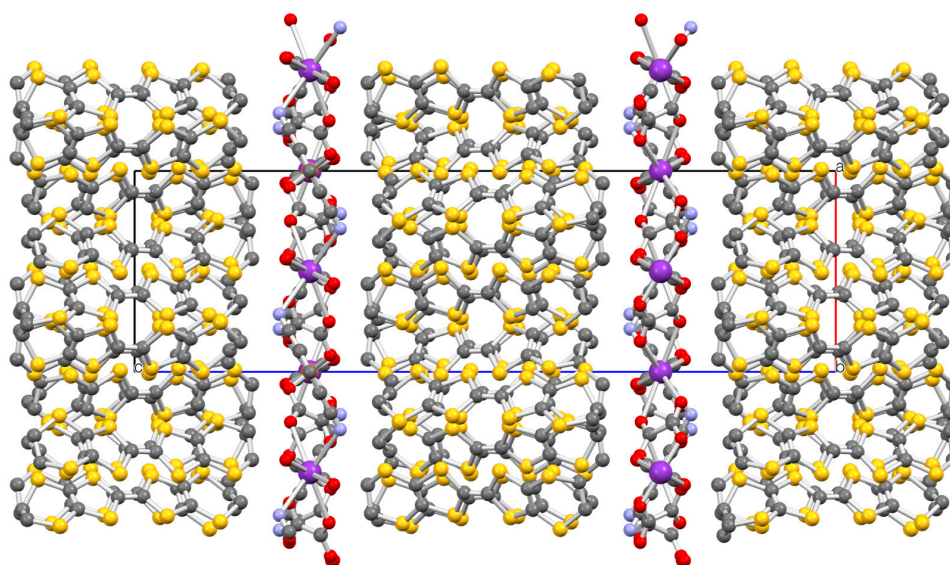
Figure 2. View of the cationic and anionic layers alternating along the *c*-direction in **1**.

The anionic layers form a honeycomb structure with hexagonal cavities that are occupied by the benzonitrile guest molecules (Figure 3a). The –CN group of the benzonitrile molecule presents a disorder over two positions related by the C_2 axis passing through the centre of the aromatic ring. The –CN group in both positions lies very close to a K^+ cation (K1-N100 = 3.055(15) Å) and, therefore, we can consider that the K^+ ions present a 6 + 2 coordination. This double orientation of the –CN groups and the close distance from the N atom to the monovalent cation is also observed in all the other reported orthorhombic structures with PhCN as solvent (Table 2) [7,32,47]. The Mn···K distances (6.308, 6.239 and 6.308 Å) reflect a slight elongation of the hexagonal cavities parallel to the C_2 axis to accommodate the –CN group of the PhCN guest molecule. Similar elongations are also observed in all the reported orthorhombic $(ET)_4[AM(C_2O_4)_3]\cdot G$ phases except in the Al-NH_4^+ and Ru-H_3O^+/K^+ compounds.
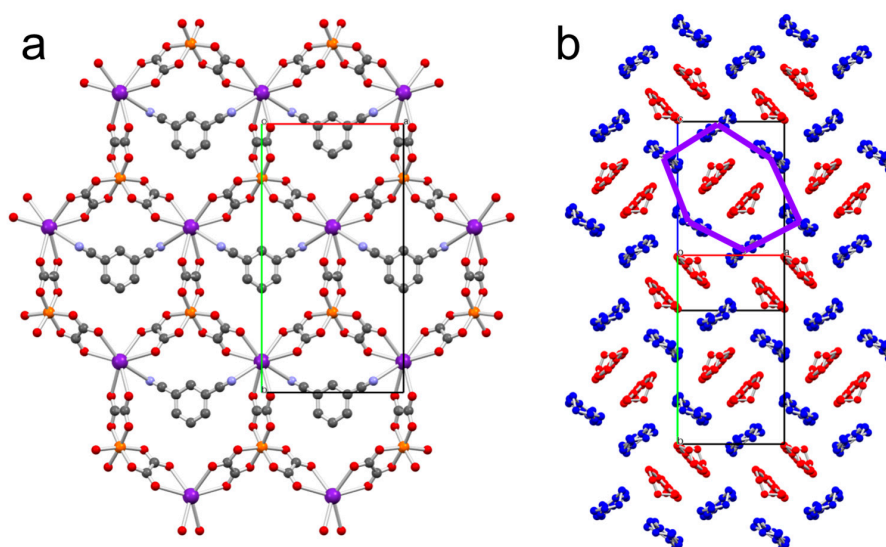

Figure 3. Structure of compound **1**: (**a**) view of the anionic layer showing the two possible positions of the –CN groups and the K–N bond. (**b**) view of the pseudo-κ packing of the bis(ethylenedithio)tetrathiafulvalene (ET) molecules in the cationic layer showing the A-type dimers (in red) surrounded by six B-type monomers (in blue). H atoms have been omitted for clarity.

The cationic layers are formed by ET dimers surrounded by six ET monomers in the so-called pseudo-κ phase (Figure 3b). The ET dimers are formed by A-type ET molecules, whereas the isolated ET molecules correspond to the B-type ones. As observed in other similar pseudo-κ phases, there are several short S⋯S contacts shorter that the sum of the Van der Waals radii (3.60 Å) (Table 6).
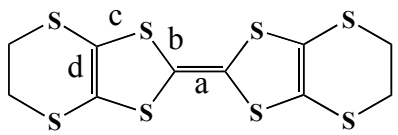
Table 6. Intermolecular S⋯S contacts shorter that the sum of the Van der Waals radii in **1**.

Atoms	Distance (Å)	Atoms	Distance (Å)
S6A[i]⋯S6B[ii]	3.563	S3A[ii]⋯S7B[i]	3.294
S8A[i]⋯S8B[ii]	3.571	S5A[ii]⋯S5B[i]	3.446
S2A[i]⋯S8B[iii]	3.497	S7A[ii]⋯S7B[i]	3.539
S8A[i]⋯S2B[iii]	3.564	-	-

Symmetry codes: i = $1.5 - x, 1.5 - y, -1/2 + z$; ii = $1 - x, y, 1.5 - z$; iii = $x, 1 - y, -1/2 + z$.

The estimation of the charge on the ET molecules in compound **1** using the formula proposed by Guionneau et al. [65] gives values of ca. +1 and ca. 0 for A- and B-type ET molecules (Table 7), respectively, as also found in all the reported orthorhombic $(ET)_4[AM(C_2O_4)_3]\cdot G$ phases [7,32,34,47,51].

Table 7. Bond distances (Å) and calculated charges of the ET molecules in **1** and **2**.

Compound	Molecule	a	b	c	d	δ	Q
1	A	1.392	1.723	1.7468	1.3415	0.7363	0.85
	B	1.353	1.7542	1.7565	1.337	0.8207	0.22
2	A	1.424	1.694	1.718	1.380	0.6080	1.81

$\delta = (b + c) - (a + d)$; $Q = 6.347 - 7.463 \times \delta$.

Structure of $(ET)[Mn^{II}Cl_4]\cdot H_2O$ (**2**). Compound **2** crystallizes in the orthorhombic space group *Pnna* (Table 5). The asymmetric unit contains a half ET molecule, half $[MnCl_4]^{2-}$ anion and half water molecule lying on special positions. Figure 4 shows the ellipsoid diagram of the molecules in **2** together with the atom-labelling scheme.
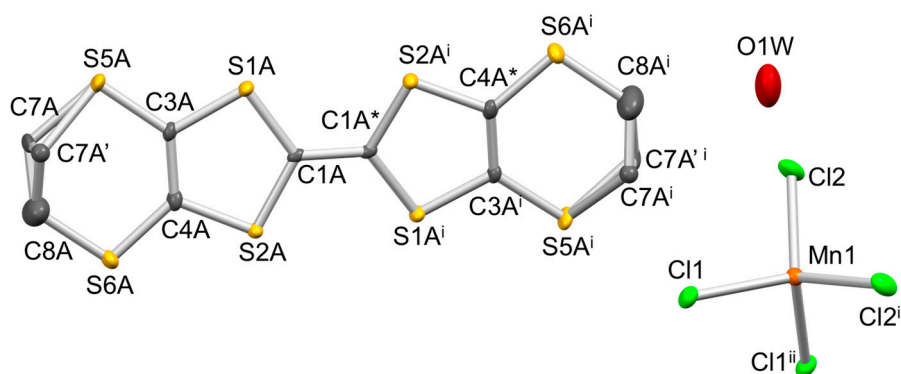

Figure 4. Thermal ellipsoid diagram (at 50% probability) of the molecules in compound **2**. Symmetry code: i = $1/2 - x, -y, z$; ii = $x, 1.5 - y, 1.5 - z$.

The crystal structure of compound **2** consists of layers of ET molecules lying parallel to the plane alternating with layers of $[MnCl_4]^{2-}$ anions (Figure 5a,d). The anions adopt a square lattice with

Mn···Mn distances of 8.321 Å (Figure 5b) and with a shortest Cl···Cl intermolecular contact of 4.877 Å, well above the sum of the Van der Waals radii (3.50 Å). The cationic layer contains ET molecules lying parallel to the layer forming double layers. The ET molecules are parallel to each other inside the double layers but are orthogonal to the ET molecules of consecutive double layers (Figure 5c). This very unusual packing of the ET molecules parallel to the layer may be due to the +2 charge of the ET molecules (Table 7), precluding the usual packing in columns or dimers due to the coulombic repulsions. The short anion–cation contacts in **2** (Table 8) are also a consequence of this double charge on the ET molecules. Additionally, there is a Cl···O short contact (3.336 Å) that suggests the presence of hydrogen bonds of the type O–H···Cl connecting neighbouring $[MnCl_4]^{2-}$ anions. Unfortunately, the H atoms of the water molecules could not be located in the single crystal structural analysis.
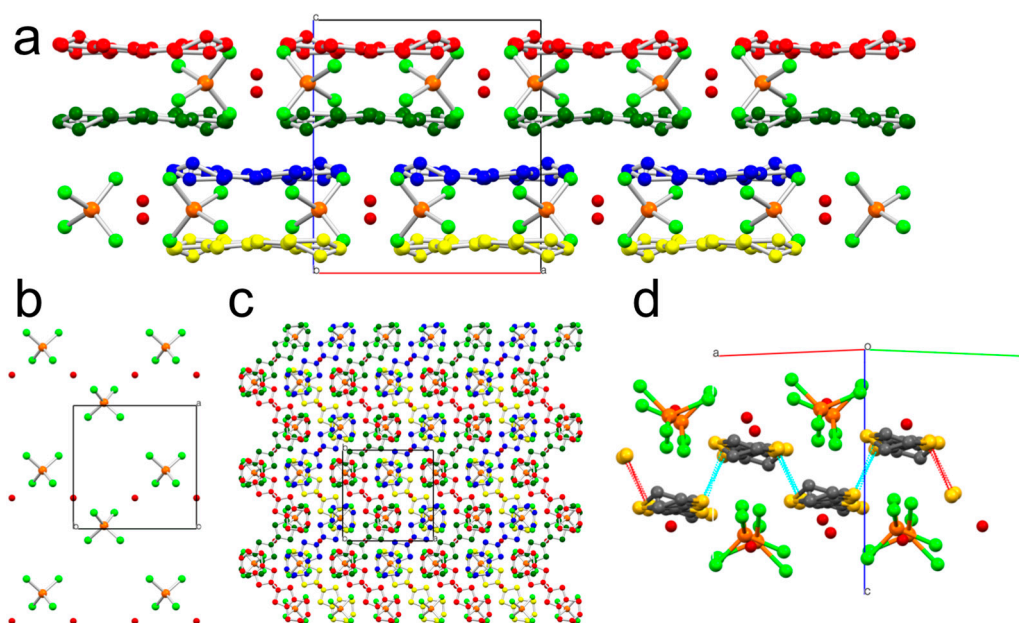

Figure 5. Structure of compound **2**: (**a**) view of the cationic and anionic layers alternating along the *c* direction in **2**. Green and blue (or red and yellow) ET molecules form one double layer; (**b**) view of the anionic layer; (**c**) view of two consecutive double ET and anionic layers down the *c* direction; (**d**) view of the zigzag chains in the *ab* plane showing the short S···S intermolecular contacts.

Table 8. Cation–anion contacts shorter than the sum of the Van der Waals radii in **2**.

Atoms	Distance (Å)	Atoms	Distance (Å)	Atoms	Distance (Å)
Cl1-S5A	3.250	Cl1^{ii}-S2A^{iii}	3.417	S2A^{v}-S2A^{vi}	3.412
Cl1-C7A′	3.437	Cl2^{ii}-S2A^{iii}	3.446	S2A^{v}-S6A^{vi}	3.597
Cl1-S1A^{i}	3.353	Cl2^{ii}-S6A^{iv}	3.295	C7A$'^{v}$-O1W^{vii}	3.147

Symmetry codes: i = 1/2 − *x*, 1 − *y*, *z*; ii = *x*, 1.5 − *y*, 1.5 − *z*; iii = *x*, 1 + *y*, *z*; iv = 1.5 − *x*, 1 − *y*, *z*; v = 1/2 − *x*, −*y*, *z*; vi = −1/2 + *x*, *y*, 1 − *z*; vii = −1 + *x*, −1 + *y*, *z*.

The presence of ET^{2+} di-cations is very unusual. In fact, only six ET salts with ET^{2+} di-cations have been reported to date [66–69]. Its presence in **2** implies that the anion must be $[MnCl_4]^{2-}$, i.e., that the precursor Mn(III) salt has been reduced to Mn(II). The oxidation state of the Mn ion in this anion is confirmed by the magnetic measurements (see below) and by the Mn–Cl bond distances in the anion (Mn1–Cl1 = 2.3724 (15) Å and Mn1–Cl2 = 2.3638 (15) Å). These distances are very similar to those reported for the $[Mn^{II}Cl_4]^{2-}$ dianion in all the reported ET salts with this anion (2.348–2.363 Å, Table 9). Furthermore, the hypothetical $[Mn^{III}Cl_4]^{-}$ monoanion has never been reported and the Mn–Cl bond distances should be ca. 0.2 Å shorter, (i.e., around 2.15–2.17 Å).

Table 9. Average Mn–Cl bond distances (Å) in all the ET salts with the $[MnCl_4]^{2-}$ anion.

Compound	Formula	Mn–Cl (Å)	Ref
ECIQEM	β''-(ET)$_3$MnCl$_4$·TCE	2.360	[70]
FEWJAT	α-(ET)$_7$[MnCl$_4$]$_2$·TCE	2.348	[71]
GAMSOC	(ET)$_3$[MnCl$_4$]$_2$	2.363	[67]
2	(ET)[MnCl$_4$]·H$_2$O	2.368	this work

TCE = 1,1,2-trichloroethane = CCl$_2$HCClH$_2$.

2.3. Magnetic Properties

The product of the magnetic susceptibility times the temperature ($\chi_m T$) per Mn(III) ion for compound **1** shows a value of ca. 3.2 cm^3·K·mol^{-1}, close to the expected one (3.0 cm^3·K·mol^{-1}) for an $S = 2$ isolated Mn(III) ion with $g = 2$ (Figure 6). When the temperature is lowered, $\chi_m T$ remains constant down to ca. 50 K where a progressive decrease starts to reach a value of ca. 1.0 cm^3·K·mol^{-1} at 2 K. This behaviour indicates that compound **1** is essentially paramagnetic and presents the contribution expected for the anionic lattice, in agreement with the crystal structure that shows magnetically isolated $[Mn(C_2O_4)_3]^{3-}$ anions since the K$^+$ ions are diamagnetic. The decrease at low temperatures is simply due to the presence of a zero field splitting of the $S = 2$ spin ground state. The lack of magnetic contribution of the cationic lattice indicates that the spins on the ET molecules of the (ET$_2$)$^{2+}$ dimers are strongly antiferromagnetically coupled and the neutral isolated ET monomers are also diamagnetic.
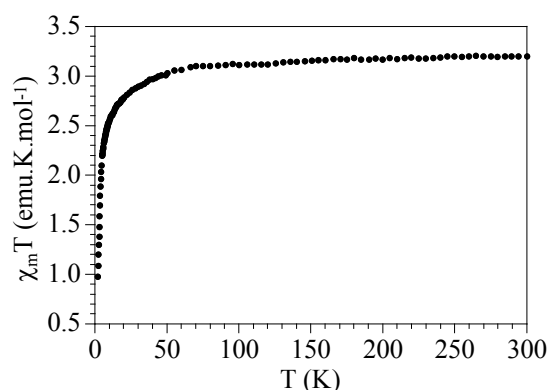
Figure 6. Thermal variation of the $\chi_m T$ product per Mn(III) ion for compound **1**.

For compound **2**, the $\chi_m T$ product per $[MnCl_4]^{2-}$ anion shows a value of ca. 4.5 cm^3·K·mol^{-1}, close to the expected one (4.375 cm^3·K·mol^{-1}) for an $S = 5/2$ isolated Mn(II) ion with $g = 2$ (Figure 7). When the sample is cooled, $\chi_m T$ shows a progressive decrease to reach a value of ca. 1.0 cm^3·K·mol^{-1} at 2 K. This behaviour indicates that compound **2** presents a weak antiferromagnetic coupling that might be attributed to a relatively short intermolecular Cl···Cl contact (4.877 Å) or to the short O–H···Cl H-bonds present in the anionic layer. Note that weak antiferromagnetic couplings through Cl···H–N contacts with similar distances have already been observed and confirmed with theoretical calculations [72]. Accordingly, we have fit the magnetic properties to a simple Curie–Weiss law [$\chi = C/(T - \theta)$] in order to estimate the weak magnetic coupling in **1**. Thus, the χ_m^{-1} vs. T plot can be fit in the 30–300 K range with a Curie constant, $C = 4.57$ cm^3·K·mol^{-1} and a Weiss temperature, $\theta = -9.4$ cm^{-1} (solid line in insert in Figure 7), confirming the presence of a weak antiferromagnetic coupling. As in **1**, we do not observe any magnetic contribution of the cationic lattice, suggesting that, as expected, the ET^{2+} cations are diamagnetic.
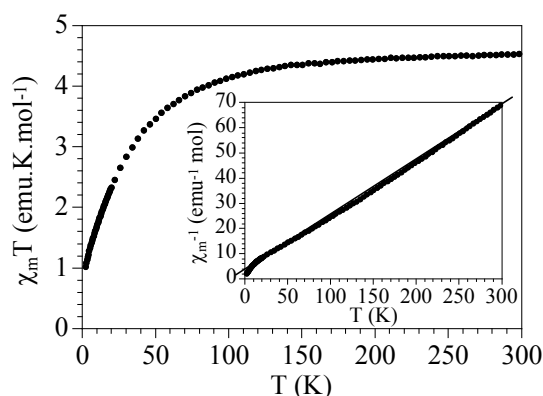
Figure 7. Thermal variation of the $\chi_m T$ product per $[MnCl_4]^{2-}$ ion for **2**. Inset shows the Curie–Weiss fit.

2.4. Electrical Properties

Compound **1** is a semiconductor with a room temperature conductivity value of ca. 2×10^{-5} S/cm and an activation energy of ca. 180 meV (Figure 8). This behaviour is very similar to that observed in all the similar orthorhombic salts of the type $(ET)_4[AM(C_2O_4)_3]\cdot G$ that are semiconductors with activation energies in the range 140–225 meV (Table 2). The semiconducting behaviour is attributed to the presence of completely ionized $(ET_2)^{2+}$ dimers surrounded by neutral ET monomers.

Compound **2** is also a semiconductor with a conductivity at room temperature of ca. 8×10^{-5} S/cm and an activation energy of ca. 210 meV (Figure 8). Note that this behaviour can be attributed to two possible reasons: (i) a charge transfer between the Cl ligands of the $[MnCl_4]^{2-}$ anion through the six short Cl···S contacts (see Table 8); and (ii) the presence of a small degree of mixed valence in the ET molecules due to the presence of neutral or (most probably) mono-cationic ET molecules. Although most of the ET molecules are doubly oxidized, we cannot discard that, during the electro-crystallization process, some mono cationic ET^+ molecules enter in the structure. This is in agreement with the average charge of ca. 1.8 found for the ET molecules in **2** (see Table 7). The weak electron delocalization would take place through the two short S···S intermolecular contacts present in compound **2** (Figure 5d and Table 8).
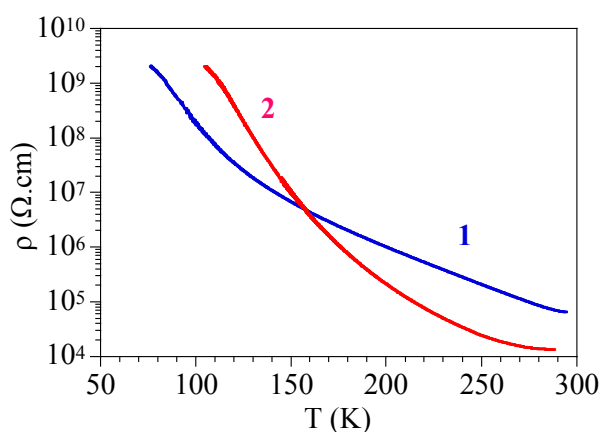

Figure 8. Thermal variation of the electrical resistivity of compounds **1** and **2**.

3. Experimental Section

3.1. Starting Materials

The organic donor bis(ethylenedithio)tetrathiafulvalene (ET), the 18-crown-6 ether, benzoic acid and all the solvents used in this work are commercially available and were used as received.

The potassium salt $K_3[Mn(C_2O_4)_3]$ was prepared as previously reported [73] and was recrystallized several times from water. The radical salts were prepared by electrochemical oxidation of ET on platinum wire electrodes (1 mm diameter) in U-shaped cells under low constant current (Table 10). The anodic and cathodic compartments are separated by a porous glass frit. The exact conditions for the synthesis of each particular radical salt are described in Table 10.

Table 10. Synthetic conditions used for salts **1** and **2**.

Compound	Anode	Cathode	Current	Time
$(ET)_4[KMn(C_2O_4)_3]\cdot PhCN$ (**1**)	ET (10 mg) PhCN (10 mL) MeOH (1 mL)	$K_3[Mn(C_2O_4)_3]$ (0.1 mmol) 18-crown-6 (90 mg) PhCOOH (0.147 mmol) PhCN (10 mL) MeOH (1.5 mL)	3 μA	1 week
$(ET)[MnCl_4]\,H_2O$ (**2**)	ET (10 mg) TCE (10 mL) MeOH (1 mL)	$K_3[Mn(C_2O_4)_3]$ (0.1 mmol) 18-crown-6 (90 mg) TCE (10 mL) MeOH (1 mL)	2 μA 4 μA 5 μA	3 weeks 1 week 1 week

TCE = 1,1,2-trichloroethane = CCl_2HCClH_2.

3.2. Synthesis of $(ET)_4[KMn(C_2O_4)_3]\cdot PhCN$ (**1**)

A solution of racemic $K_3[Mn(C_2O_4)_3]$ (43.6 mg, 0.1 mmol), PhCOOH (18 mg, 0.15 mmol) and 18-crown-6 ether (90 mg, 0.35 mmol) in a mixture of 10 mL of PhCN and 1.5 mL of MeOH was placed in the cathode of a U-shaped electrochemical cell. A solution of ET (10 mg, 0.026 mmol) in a mixture of 10 mL of PhCN and 1.5 mL of MeOH was placed in the anode of the U-shaped cell and a constant current of 3 μA was applied. Black plate single crystals were collected from the anode after one week.

3.3. Synthesis of $(ET)[MnCl_4]\cdot H_2O$ (**2**)

A solution of racemic $K_3[Mn(C_2O_4)_3]$ (43.6 mg, 0.1 mmol) and 18-crown-6 ether (90 mg, 0.35 mmol) in a mixture of 10 mL of 1,1,2-trichloroethane and 1.5 mL of MeOH was placed in the cathode of a U-shaped electrochemical cell. A solution of ET (10 mg, 0.026 mmol) in a mixture of 10 mL of 1,1,2-trichloroethane and 1.5 mL of MeOH was placed in the anode of the U-shaped cell and a constant current of 2 μA was applied during three weeks. The intensity was increased to 4 μA for one week more and finally to 5 μA. Dark green prismatic crystals were collected from the anode after one week at 5 μA.

3.4. Physical Measurements

Magnetic susceptibility measurements were carried out in the temperature range 2–300 K with an applied magnetic field of 0.5 T on polycrystalline samples of compounds **1** and **2** with a MPMS-XL-5 SQUID susceptometer (Quantum Desing, San Diego, CA, USA). The susceptibility data were corrected for the sample holders previously measured using the same conditions and for the diamagnetic contributions of the salt as deduced by using Pascal's constant tables [74].

The temperature dependence of the DC electrical conductivity was measured with the four contact method on different single crystals of compounds **1** and **2** in cooling and warming scans with similar results within experimental errors. The contacts were made with Pt wires (25 μm diameter) using graphite paste. The samples were measured in a PPMS-9 equipment (Quantum Desing, San Diego, CA, USA) connected to an external voltage source model 2450 source-meter (Keithley, Cleveland, OH, USA) and amperometer model 6514 electrometer (Keithley, Cleveland, OH, USA). The conductivity quoted values have been measured in the voltage range where the crystals are Ohmic conductors. The cooling and warming rates were 1 and 2 K·min^{-1}.

3.5. Crystallographic Data Collection and Refinement

Suitable single crystals of compounds **1** and **2** were mounted on a glass fibre using a viscous hydrocarbon oil to coat the crystal and then transferred directly to the cold nitrogen stream for data collection. X-ray data were collected at 120 K on a Supernova diffractometer (Agilent, Santa Clara, CA, USA) equipped with a graphite-monochromated Enhance (Mo) X-ray Source (λ = 0.71073 Å). The program CrysAlisPro v38.43, (Rigaku, Tokyo, Japan), was used for unit cell determinations and data reduction. Empirical absorption correction was performed using spherical harmonics, implemented in the SCALE3 ABSPACK scaling algorithm. Crystal structures were solved with direct methods with the SIR97 program [75], and refined against all F^2 values with the SHELXL-2014 program [76], using the WinGX graphical user interface [77]. All non-hydrogen atoms were refined anisotropically, and hydrogen atoms were placed in calculated positions and refined isotropically with a riding model. There is a disorder in the CH_3CN solvent molecules that appears with two possible orientations with a common N atom located on a C_2 axis. Data collection and refinement parameters are given in Table 5.

CCDC-1527866 and 1527859 contain the supplementary crystallographic data for compounds **1** and **2**, respectively. These data can be obtained free of charge from The Cambridge Crystallographic Data Centre at www.ccdc.cam.ac.uk/data_request/cif.

4. Conclusions

The combination of the magnetic anion $[Mn(C_2O_4)_3]^{3-}$ with the organic donor ET under different synthetic conditions has resulted in the synthesis of two very original magnetic and conducting radical salts: $(ET)_4[KMn(C_2O_4)_3]\cdot PhCN$ (**1**) and $(ET)[MnCl_4]\cdot H_2O$ (**2**). The radical salt with the anion $[Mn(C_2O_4)_3]^{3-}$ is the first reported member with Mn(III) of the Day's huge family of magnetic conductors and superconductors formulated as $(ET)_4[A^I M^{III}(C_2O_4)_3]\cdot G$ (A^I = H_3O^+, K^+, NH_4^+, Na^+, ...; M^{III} = Fe, Cr, Ga, Co, Al and Ru; G = PhCN, PhNO$_2$, PhCl, PhBr, py, ...). This compound crystallizes in an orthorhombic pseudo-κ phase where $(ET_2)^{2+}$ dimers are surrounded by isolated neutral ET monomers. The change of PhCN by 1,1,2-trichloroethane as a solvent gives rise to the radical salt $(ET)[MnCl_4]\cdot H_2O$, where the ET molecules have been oxidized to a very unusual oxidation state of +2 and the Mn(III) metal atom has been reduced to Mn(II). The degradation of the chlorinated solvent furnishes the Cl^- ligands for the in situ formation of the anion $[MnCl_4]^{2-}$. Both salts are semiconductors (with activation energies of ca. 180 and ca. 210 meV, respectively) and paramagnetic with magnetic moments corresponding to the anionic complexes, since the organic lattices do not contribute to the magnetic moment.

Author Contributions: S.B. designed the synthesis and performed the X-ray structural analysis. Y.S.-M. performed the synthesis of the precursor salts and of the radical salts. C.J.G.-G. performed the magnetic and conductivity measurements. All authors contributed to the writing of the manuscript.

Conflicts of Interest: The authors declare no conflict of interest.

References

1. Coronado, E.; Day, P. Magnetic Molecular Conductors. *Chem. Rev.* **2004**, *104*, 5419–5448. [CrossRef] [PubMed]
2. Enoki, T.; Miyazaki, A. Magnetic TTF-Based Charge-Transfer Complexes. *Chem. Rev.* **2004**, *104*, 5449–5478. [CrossRef] [PubMed]
3. Kobayashi, H.; Cui, H.; Kobayashi, A. Organic Metals and Superconductors Based on BETS (BETS = Bis(ethylenedithio)tetraselenafulvalene). *Chem. Rev.* **2004**, *104*, 5265–5288. [CrossRef] [PubMed]
4. Coronado, E.; Galán-Mascarós, J.R.; Gómez-García, C.J.; Laukhin, V. Coexistence of ferromagnetism and metallic conductivity in a molecule-based layered compound. *Nature* **2000**, *408*, 447–449. [CrossRef] [PubMed]

5. Kobayashi, H.; Kobayashi, A.; Cassoux, P. BETS as a source of molecular magnetic superconductors (BETS = bis(ethylenedithio)tetraselenafulvalene). *Chem. Soc. Rev.* **2000**, *29*, 325–333. [CrossRef]

6. Graham, A.W.; Kurmoo, M.; Day, P. β''-(bedt-ttf)$_4$[(H$_2$O)Fe(C$_2$O$_4$)$_3$]·PhCN: The first molecular superconductor containing paramagnetic metal ions. *J. Chem. Soc. Chem. Commun.* **1995**, 2061–2062. [CrossRef]

7. Kurmoo, M.; Graham, A.W.; Day, P.; Coles, S.J.; Hursthouse, M.B.; Caulfield, J.L.; Singleton, J.; Pratt, F.L.; Hayes, W. Superconducting and Semiconducting Magnetic Charge Transfer Salts: (BEDT-TTF)$_4$$A$Fe(C$_2O_4$)$_3$·C$_6H_5$CN ($A$ = H$_2$O, K, NH$_4$). *J. Am. Chem. Soc.* **1995**, *117*, 12209–12217. [CrossRef]

8. Kobayashi, H.; Fujiwara, E.; Fujiwara, H.; Tanaka, H.; Tamura, I.; Bin, Z.; Gritsenko, V.; Otsuka, T.; Kobayashi, A.; Tokumoto, M.; et al. Magnetic organic superconductors based on BETS molecules—Interplay of conductivity and magnetism. *Mol. Cryst. Liq. Cryst.* **2002**, *379*, 9–18. [CrossRef]

9. Kobayashi, H.; Tomita, H.; Naito, T.; Kobayashi, A.; Sakai, F.; Watanabe, T.; Cassoux, P. New BETS conductors with magnetic anions (BETS = bis(ethylenedithio)-tetraselenafulvalene). *J. Am. Chem. Soc.* **1996**, *118*, 368–377. [CrossRef]

10. Kobayashi, H.; Fujiwara, E.; Fujiwara, H.; Tanaka, H.; Otsuka, T.; Kobayashi, A.; Tokumoto, M.; Cassoux, P. Antiferromagnetic organic superconductors, BETS$_2$FeX_4 (X = Br, Cl). *Mol. Cryst. Liq. Cryst.* **2002**, *380*, 139–144. [CrossRef]

11. Fujiwara, H.; Fujiwara, E.; Nakazawa, Y.; Narymbetov, B.Z.; Kato, K.; Kobayashi, H.; Kobayashi, A.; Tokumoto, M.; Cassoux, P. A novel antiferromagnetic organic superconductor κ-(BETS)$_2$FeBr$_4$ [where BETS = bis(ethylenedithio)tetraselenafulvalene]. *J. Am. Chem. Soc.* **2001**, *123*, 306–314. [CrossRef] [PubMed]

12. Kobayashi, H.; Tanaka, H.; Ojima, E.; Fujiwara, H.; Nakazawa, Y.; Otsuka, T.; Kobayashi, A.; Tokumoto, M.; Cassoux, P. Antiferromagnetism and superconductivity of BETS conductors with Fe^{3+} ions. *Synth. Met.* **2001**, *120*, 663–666. [CrossRef]

13. Kobayashi, H.; Tanaka, H.; Ojima, E.; Fujiwara, H.; Otsuka, T.; Kobayashi, A.; Tokumoto, M.; Cassoux, P. Coexistence of antiferromagnetic order and superconductivity in organic conductors. *Polyhedron* **2001**, *20*, 1587–1592. [CrossRef]

14. Tanaka, H.; Kobayashi, H.; Kobayashi, A.; Cassoux, P. Superconductivity, antiferromagnetism, and phase diagram of a series of organic conductors: λ-(BETS)$_2$Fe$_x$Ga$_{1-x}$Br$_y$Cl$_{4-y}$. *Adv. Mater.* **2000**, *12*, 1685–1689. [CrossRef]

15. Ojima, E.; Fujiwara, H.; Kato, K.; Kobayashi, H.; Tanaka, H.; Kobayashi, A.; Tokumoto, M.; Cassoux, P. Antiferromagnetic organic metal exhibiting superconducting transition, κ-(BETS)$_2$FeBr$_4$ [BETS = bis(ethylenedithio)tetraselenafulvalene]. *J. Am. Chem. Soc.* **1999**, *121*, 5581–5582. [CrossRef]

16. Alberola, A.; Coronado, E.; Galán-Mascarós, J.R.; Giménez-Saiz, C.; Gómez-García, C.J. A molecular metal ferromagnet from the organic donor bis(ethylenedithio)-tetraselenafulvalene and bimetallic oxalate complexes. *J. Am. Chem. Soc.* **2003**, *125*, 10774–10775. [CrossRef] [PubMed]

17. Coronado, E.; Galán-Mascarós, J.R.; Gómez-García, C.J. Charge transfer salts of tetrathiafulvalene derivatives with magnetic iron(III) oxalate complexes: [TTF]$_7$[Fe(ox)$_3$]$_2$·4H$_2$O, [TTF]$_5$[Fe$_2$(ox)$_5$]·2PhMe·2H$_2$O and [TMTTF]$_4$[Fe$_2$(ox)$_5$]·PhCN·4H$_2$O (TMTTF = tetramethyltetrathiafulvalene). *J. Chem. Soc. Dalton Trans.* **2000**, 205–210. [CrossRef]

18. Coronado, E.; Galán-Mascarós, J.R.; Giménez-Saiz, C.; Gómez-García, C.J.; Martínez-Agudo, J.M.; Martínez-Ferrero, E. Magnetic properties of hybrid molecular materials based on oxalato complexes. *Polyhedron* **2003**, *22*, 2381–2386. [CrossRef]

19. Coronado, E.; Curreli, S.; Giménez-Saiz, C.; Gómez-García, C.J.; Alberola, A. Radical salts of bis(ethylenediseleno)tetrathiafulvalene with paramagnetic tris(oxalato)metalate anions. *Inorg. Chem.* **2006**, *45*, 10815–10824. [CrossRef] [PubMed]

20. Martin, L.; Turner, S.S.; Day, P.; Guionneau, P.; Howard, J.A.K.; Uruichi, M.; Yakushi, K. Synthesis, crystal structure and properties of the semiconducting molecular charge-transfer salt (bedt-ttf)$_2$Ge(C$_2$O$_4$)$_3$·PhCN [bedt-ttf = bis(ethylenedithio)tetrathiafulvalene]. *J. Mater. Chem.* **1999**, *9*, 2731–2736. [CrossRef]

21. Martin, L.; Day, P.; Clegg, W.; Harrington, R.W.; Horton, P.N.; Bingham, A.; Hursthouse, M.B.; McMillan, P.; Firth, S. Multi-layered molecular charge-transfer salts containing alkali metal ions. *J. Mater. Chem.* **2007**, *17*, 3324–3329. [CrossRef]

22. Martin, L.; Day, P.; Nakatsuji, S.; Yamada, J.; Akutsu, H.; Horton, P. A molecular charge transfer salt of BEDT-TTF containing a single enantiomer of tris(oxalato)chromate(III) crystallised from a chiral solvent. *CrystEngComm* **2010**, *12*, 1369–1372. [CrossRef]

23. Martin, L.; Day, P.; Barnett, S.A.; Tocher, D.A.; Horton, P.N.; Hursthouse, M.B. Magnetic molecular charge-transfer salts containing layers of water and tris(oxalato)ferrate(III) anions. *CrystEngComm* **2008**, *10*, 192–196. [CrossRef]

24. Zhang, B.; Zhang, Y.; Liu, F.; Guo, Y. Synthesis, crystal structure, and characterization of charge-transfer salt: (BEDT-TTF)$_5$[Fe(C$_2$O$_4$)$_3$]·(H$_2$O)$_2$·CH$_2$Cl$_2$ (BEDT-TTF = bis(ethylenedithio)tetrathiafulvalene). *CrystEngComm* **2009**, *11*, 2523–2528. [CrossRef]

25. Martin, L.; Day, P.; Nakatsuji, S.; Yamada, J.; Akutsu, H.; Horton, P.N. BEDT-TTF Tris(oxalato)germanate(IV) Salts with Novel Donor Packing Motifs. *Bull. Chem. Soc. Jpn.* **2010**, *83*, 419–423. [CrossRef]

26. Rashid, S.; Turner, S.S.; Day, P.; Light, M.E.; Hursthouse, M.B. Molecular charge-transfer salt of BEDT-TTF [bis(ethylenedithio)tetrathiafulvalene] with the oxalate-bridged dimeric anion [Fe$_2$(C$_2$O$_4$)$_5$]$^{4-}$. *Inorg. Chem.* **2000**, *39*, 2426–2428. [CrossRef]

27. Coronado, E.; Galán-Mascarós, J.R.; Giménez-Saiz, C.; Gómez-García, C.J.; Ruiz-Perez, C. Hybrid organic/inorganic molecular materials formed by tetrathiafulvalene radicals and magnetic trimeric clusters of dimetallic oxalate-bridged complexes: The series (TTF)$_4$\{M^{II}(H$_2$O)$_2$[M^{III}(ox)$_3$]$_2$\}·nH$_2$O (M^{II} = Mn, Fe, Co, Ni, Cu and Zn; M^{III} = Cr and Fe; ox = C$_2$O$_4$$^{2-}$). *Eur. J. Inorg. Chem.* **2003**, 2290–2298. [CrossRef]

28. Coronado, E.; Galán-Mascarós, J.R.; Giménez-Saiz, C.; Gómez-García, C.J.; Ruiz-Pérez, C.; Triki, S. Hybrid molecular materials formed by alternating layers of bimetallic oxalate complexes and tetrathiafulvalene molecules: Synthesis, structure, and magnetic properties of TTF$_4$\{Mn(H$_2$O)$_2$[Cr(ox)$_3$]$_2$\}·14H$_2$O. *Adv. Mater.* **1996**, *8*, 737–740. [CrossRef]

29. Alberola, A.; Coronado, E.; Galán-Mascarós, J.R.; Giménez-Saiz, C.; Gómez-García, C.J.; Romero, F.M. Multifunctionality in hybrid molecular materials: Design of ferromagnetic molecular metals and hybrid magnets. *Synth. Met.* **2003**, *133*, 509–513. [CrossRef]

30. Galán-Mascarós, J.R.; Coronado, E.; Goddard, P.A.; Singleton, J.; Coldea, A.I.; Wallis, J.D.; Coles, S.J.; Alberola, A. A Chiral Ferromagnetic Molecular Metal. *J. Am. Chem. Soc.* **2010**, *132*, 9271–9273. [CrossRef] [PubMed]

31. Coronado, E.; Galán-Mascarós, J.R. Hybrid molecular conductors. *J. Mater. Chem.* **2005**, *15*, 66–74. [CrossRef]

32. Martin, L.; Turner, S.S.; Day, P.; Guionneau, P.; Howard, J.A.K.; Hibbs, D.E.; Light, M.E.; Hursthouse, M.B.; Uruichi, M.; Yakushi, K. Crystal Chemistry and Physical Properties of Superconducting and Semiconducting Charge Transfer Salts of the Type (BEDT-TTF)$_4$[$A^I M^{III}$(C$_2$O$_4$)$_3$]·PhCN (A^I = H$_3$O, NH$_4$, K; M^{III} = Cr, Fe, Co, Al; BEDT-TTF = Bis(ethylenedithio)tetrathiafulvalene). *Inorg. Chem.* **2001**, *40*, 1363–1371. [CrossRef] [PubMed]

33. Akutsu-Sato, A.; Akutsu, H.; Yamada, J.; Nakatsuji, S.; Turner, S.S.; Day, P. Suppression of superconductivity in a molecular charge transfer salt by changing guest molecule: β″-(BEDT-TTF)$_4$[(H$_3$O)Fe(C$_2$O$_4$)$_3$] (C$_6$H$_5$CN)$_x$(C$_5$H$_5$N)$_{1-x}$. *J. Mater. Chem.* **2007**, *17*, 2497–2499. [CrossRef]

34. Prokhorova, T.G.; Buravov, L.I.; Yagubskii, E.B.; Zorina, L.V.; Khasanov, S.S.; Simonov, S.V.; Shibaeva, R.P.; Korobenko, A.V.; Zverev, V.N. Effect of electrocrystallization medium on quality, structural features, and conducting properties of single crystals of the (BEDT-TTF)$_4 A^I$[Fe^{III}(C$_2$O$_4$)$_3$]·G family. *CrystEngComm* **2011**, *13*, 537–545. [CrossRef]

35. Turner, S.S.; Day, P.; Malik, K.M.A.; Hursthouse, M.B.; Teat, S.J.; MacLean, E.J.; Martin, L.; French, S.A. Effect of included solvent molecules on the physical properties of the paramagnetic charge transfer salts β″-(bedt-ttf)$_4$[(H$_3$O)Fe(C$_2$O$_4$)$_3$]·solvent (bedt-ttf = bis(ethylenedithio)tetrathiafulvalene). *Inorg. Chem.* **1999**, *38*, 3543–3549. [CrossRef] [PubMed]

36. Rashid, S.; Turner, S.S.; Day, P.; Howard, J.A.K.; Guionneau, P.; McInnes, E.J.L.; Mabbs, F.E.; Clark, R.J.H.; Firth, S.; Biggs, T. New superconducting charge-transfer salts (BEDT-TTF)$_4$[A·M(C$_2$O$_4$)$_3$]·C$_6$H$_5$NO$_2$ (A = H$_3$O or NH$_4$, M = Cr or Fe, BEDT-TTF = bis(ethylenedithio)tetrathiafulvalene). *J. Mater. Chem.* **2001**, *11*, 2095–2101. [CrossRef]

37. Sun, S.Q.; Wu, P.J.; Zhang, Q.C.; Zhu, D.B. The New Semiconducting Magnetic Charge Transfer Salt (BEDT-TTF)$_4$·H$_2$O·Fe(C$_2$O$_4$)$_3$·C$_6$H$_5$NO$_2$: Crystal Structure and Physical Properties. *Mol. Cryst. Liq. Cryst.* **1998**, *319*, 259–269. [CrossRef]

38. Sun, S.; Wu, P.; Zhang, Q.; Zhu, D. The new semiconducting magnetic charge transfer salt (BEDT-TTF)$_4$·H$_2$O·Fe(C$_2$O$_4$)$_3$·C$_6$H$_5$NO$_2$: Crystal structure and physical properties. *Synth. Met.* **1998**, *94*, 161–166. [CrossRef]

39. Zorina, L.; Prokhorova, T.; Simonov, S.; Khasanov, S.; Shibaeva, R.; Manakov, A.; Zverev, V.; Buravov, L.; Yagubskii, E. Structure and magnetotransport properties of the new quasi-two-dimensional molecular metal β''-(BEDT-TTF)$_4$H$_3$O[Fe(C$_2$O$_4$)$_3$]·C$_6$H$_4$Cl$_2$. *J. Exp. Theor. Phys.* **2008**, *106*, 347–354. [CrossRef]

40. Coronado, E.; Curreli, S.; Giménez-Saiz, C.; Gómez-García, C.J. A novel paramagnetic molecular superconductor formed by bis(ethylenedithio)tetrathiafulvalene, tris(oxalato) ferrate(III) anions and bromobenzene as guest molecule: ET$_4$[(H$_3$O)Fe(C$_2$O$_4$)$_3$]·C$_6$H$_5$Br. *J. Mater. Chem.* **2005**, *15*, 1429–1436. [CrossRef]

41. Prokhorova, T.G.; Khasanov, S.S.; Zorina, L.V.; Buravov, L.I.; Tkacheva, V.A.; Baskakov, A.A.; Morgunov, R.B.; Gener, M.; Canadell, E.; Shibaeva, R.P.; et al. Molecular Metals Based on BEDT-TTF Radical Cation Salts with Magnetic Metal Oxalates as Counterions: β''-(BEDT-TTF)$_4$A[M(C$_2$O$_4$)$_3$]·DMF (A = NH$_4^+$, K$^+$; M = Cr^{III}, Fe^{III}). *Adv. Funct. Mater.* **2003**, *13*, 403–411. [CrossRef]

42. Zorina, L.V.; Khasanov, S.S.; Simonov, S.V.; Shibaeva, R.P.; Bulanchuk, P.O.; Zverev, V.N.; Canadell, E.; Prokhorova, T.G.; Yagubskii, E.B. Structural phase transition in the β''-(BEDT-TTF)$_4$H$_3$O[Fe(C$_2$O$_4$)$_3$]·*G* crystals (where *G* is a guest solvent molecule). *CrystEngComm* **2012**, *14*, 460–465. [CrossRef]

43. Coronado, E.; Curreli, S.; Giménez-Saiz, C.; Gómez-García, C.J. The series of molecular conductors and superconductors ET$_4$[AFe(C$_2$O$_4$)$_3$]·PhX (ET = bis(ethylenedithio)tetrathiafulvalene; (C$_2$O$_4$)$^{2-}$ = oxalate; A$^+$ = H$_3$O$^+$, K$^+$; X = F, Cl, Br, and I): Influence of the halobenzene guest molecules on the crystal structure and superconducting properties. *Inorg. Chem.* **2012**, *51*, 1111–1126. [PubMed]

44. Akutsu-Sato, A.; Kobayashi, A.; Mori, T.; Akutsu, H.; Yamada, J.; Nakatsuji, S.; Turner, S.S.; Day, P.; Tocher, D.A.; Light, M.E.; et al. Structures and Physical Properties of New β'-BEDT-TTF Tris-Oxalatometallate (III) Salts Containing Chlorobenzene and Halomethane Guest Molecules. *Synth. Met.* **2005**, *152*, 373–376. [CrossRef]

45. Coronado, E.; Curreli, S.; Gimenez-Saiz, C.; Gómez-García, C.J. New magnetic conductors and superconductors based on BEDT-TTF and BEDS-TTF. *Synth. Met.* **2005**, *154*, 245–248. [CrossRef]

46. Kanehama, R.; Yoshino, Y.; Ishii, T.; Manabe, T.; Hara, H.; Miyasaka, H.; Matsuzaka, H.; Yamashita, M.; Katada, M.; Nishikawa, H.; et al. Syntheses and physical properties of new charge-transfer salts consisting of a conducting BEDT-TTF column and magnetic 1D or 2D Fe(III) networks. *Synth. Met.* **2003**, *133*, 553–554. [CrossRef]

47. Martin, L.; Turner, S.S.; Day, P.; Malik, K.M.A.; Coles, S.J.; Hursthouse, M.B. Polymorphism based on molecular stereoisomerism in tris(oxalato) Cr(III) salts of bedt-ttf [bis(ethylenedithio)tetrathiafulvalene]. *Chem. Commun.* **1999**, 513–514. [CrossRef]

48. Rashid, S.; Turner, S.S.; Le Pevelen, D.; Day, P.; Light, M.E.; Hursthouse, M.B.; Firth, S.; Clark, R.J.H. β''-(BEDT-TTF)$_4$[(H$_3$O)Cr(C$_2$O$_4$)$_3$]CH$_2$Cl$_2$: Effect of included solvent on the structure and properties of a conducting molecular charge-transfer salt. *Inorg. Chem.* **2001**, *40*, 5304–5306. [CrossRef] [PubMed]

49. Akutsu, H.; Akutsu-Sato, A.; Turner, S.S.; Le Pevelen, D.; Day, P.; Laukhin, V.; Klehe, A.; Singleton, J.; Tocher, D.A.; Probert, M.R.; et al. Effect of included guest molecules on the normal state conductivity and superconductivity of β''-(ET)$_4$[(H$_3$O)Ga(C$_2$O$_4$)$_3$]·*G* (*G* = pyridine, nitrobenzene). *J. Am. Chem. Soc.* **2002**, *124*, 12430–12431. [CrossRef] [PubMed]

50. Prokhorova, T.G.; Buravov, L.I.; Yagubskii, E.B.; Zorina, L.V.; Simonov, S.V.; Shibaeva, R.P.; Zverev, V.N. Metallic Bi- and Monolayered Radical Cation Salts Based on Bis(ethylenedithio)-tetrathiafulvalene (BEDT-TTF) with the Tris(oxalato)gallate Anion. *Eur. J. Inorg. Chem.* **2014**, 3933–3940. [CrossRef]

51. Prokhorova, T.G.; Zorina, L.V.; Simonov, S.V.; Zverev, V.N.; Canadell, E.; Shibaeva, R.P.; Yagubskii, E.B. The first molecular superconductor based on BEDT-TTF radical cation salt with paramagnetic tris(oxalato)ruthenate anion. *CrystEngComm* **2013**, *15*, 7048–7055. [CrossRef]

52. Prokhorova, T.G.; Buravov, L.I.; Yagubskii, E.B.; Zorina, L.V.; Simonov, S.V.; Zverev, V.N.; Shibaeva, R.P.; Canadell, E. Effect of Halopyridine Guest Molecules on the Structure and Superconducting Properties of β''-[Bis(ethylenedithio)tetrathiafulvalene]$_4$(H$_3$O)[Fe(C$_2$O$_4$)$_3$]·Guest Crystals. *Eur. J. Inorg. Chem.* **2015**, *2015*, 5611–5620. [CrossRef]

53. Martin, L.; Engelkamp, H.; Akutsu, H.; Nakatsuji, S.; Yamada, J.; Horton, P.; Hursthouse, M.B. Radical-cation salts of BEDT-TTF with lithium tris(oxalato)metallate(III). *Dalton Trans.* **2015**, *44*, 6219–6223. [CrossRef] [PubMed]

54. Zorina, L.V.; Khasanov, S.S.; Simonov, S.V.; Shibaeva, R.P.; Zverev, V.N.; Canadell, E.; Prokhorova, T.G.; Yagubskii, E.B. Coexistence of two donor packing motifs in the stable molecular metal α-pseudo-κ-(BEDT-TTF)$_4$(H$_3$O)[Fe(C$_2$O$_4$)$_3$]·C$_6$H$_4$Br$_2$. *CrystEngComm* **2011**, *13*, 2430–2438. [CrossRef]

55. Akutsu, H.; Akutsu-Sato, A.; Turner, S.S.; Day, P.; Canadell, E.; Firth, S.; Clark, R.J.H.; Yamada, J.; Nakatsuji, S. Superstructures of donor packing arrangements in a series of molecular charge transfer salts. *Chem. Commun.* **2004**, 18–19. [CrossRef] [PubMed]

56. Martin, L.; Day, P.; Akutsu, H.; Yamada, J.; Nakatsuji, S.; Clegg, W.; Harrington, R.W.; Horton, P.N.; Hursthouse, M.B.; McMillan, P.; et al. Metallic molecular crystals containing chiral or racemic guest molecules. *CrystEngComm* **2007**, *9*, 865–867. [CrossRef]

57. Martin, L.; Akutsu, H.; Horton, P.N.; Hursthouse, M.B.; Harrington, R.W.; Clegg, W. Chiral Radical-Cation Salts of BEDT-TTF Containing a Single Enantiomer of Tris(oxalato)aluminate(III) and -chromate(III). *Eur. J. Inorg. Chem.* **2015**, 1865–1870. [CrossRef]

58. Martin, L.; Day, P.; Horton, P.; Nakatsuji, S.; Yamada, J.; Akutsu, H. Chiral conducting salts of BEDT-TTF containing a single enantiomer of tris(oxalato)chromate(III) crystallised from a chiral solvent. *J. Mater. Chem.* **2010**, *20*, 2738–2742. [CrossRef]

59. Martin, L.; Akutsu, H.; Horton, P.N.; Hursthouse, M.B. Chirality in charge-transfer salts of BEDT-TTF of tris(oxalato)chromate(III). *CrystEngComm* **2015**, *17*, 2783–2790. [CrossRef]

60. Coldea, A.I.; Bangura, A.F.; Singleton, J.; Ardavan, A.; Akutsu-Sato, A.; Akutsu, H.; Turner, S.S.; Day, P. Fermi-surface topology and the effects of intrinsic disorder in a class of charge-transfer salts containing magnetic ions: β''-(BEDT-TTF)$_4$[(H$_3$O)M(C$_2$O$_4$)$_3$]·Y (M = Ga, Cr, Fe; Y = C$_5$H$_5$N). *Phys. Rev. B* **2004**, *69*, 085112. [CrossRef]

61. Martin, L.; Turner, S.S.; Day, P.; Mabbs, F.E.; McInnes, E.J.L. New molecular superconductor containing paramagnetic chromium (III) ions. *Chem. Commun.* **1997**, 1367–1368. [CrossRef]

62. Rosseinsky, M.J.; Kurmoo, M.; Talham, D.R.; Day, P.; Chasseau, D.; Watkin, D. A Novel Conducting Charge-Transfer Salt-(bedt-ttf)$_3$Cl$_2$·2H$_2$O. *J. Chem. Soc. Chem. Commun.* **1988**, 88–90. [CrossRef]

63. Zhang, B.; Yao, Y.X.; Zhu, D.B. A new organic conductor (BEDT-TTF)$_5$Cl$_3$(H$_2$O)$_5$. *Synth. Met.* **2001**, *120*, 671–674. [CrossRef]

64. Mori, H.; Hirabayashi, I.; Tanaka, S.; Maruyama, Y. Preparation, Crystal and Electronic Structures, and Electrical Resistivity of (BEDT-TTF)$_3$Cl$_{2.5}$(H$_5$O$_2$). *Bull. Chem. Soc. Jpn.* **1993**, *66*, 2156–2159. [CrossRef]

65. Guionneau, P.; Kepert, C.J.; Bravic, G.; Chasseau, D.; Truter, M.R.; Kurmoo, M.; Day, P. Determining the charge distribution in BEDT-TTF salts. *Synth. Met.* **1997**, *86*, 1973–1974. [CrossRef]

66. Kanehama, R.; Umemiya, M.; Iwahori, F.; Miyasaka, H.; Sugiura, K.; Yamashita, M.; Yokochi, Y.; Ito, H.; Kuroda, S.; Kishida, H.; et al. Novel ET-Coordinated Copper(I) Complexes: Syntheses, Structures, and Physical Properties (ET = BEDT-TTF = Bis(ethylenedithio)tetrathiafulvalene). *Inorg. Chem.* **2003**, *42*, 7173–7181. [CrossRef] [PubMed]

67. Mori, T.; Inokuchi, H. A BEDT-TTF Complex Including a Magnetic Anion, (BEDT-TTF)$_3$(MnCl$_4$)$_2$. *Bull. Chem. Soc. Jpn.* **1988**, *61*, 591–593. [CrossRef]

68. Shibaeva, R.P.; Lobkovskaya, R.M.; Korotkov, V.E.; Kusch, N.D.; Yagubskii, E.B.; Makova, M.K. ET cation-radical salts with metal complex anions. *Synth. Met.* **1988**, *27*, A457–A463. [CrossRef]

69. Chou, L.; Quijada, M.A.; Clevenger, M.B.; de Oliveira, G.F.; Abboud, K.A.; Tanner, D.B.; Talham, D.R. Dication Salts of the Organic Donor Bis(ethylenedithio)tetrathiafulvalene. *Chem. Mater.* **1995**, *7*, 530–534. [CrossRef]

70. Naito, T.; Inabe, T.; Takeda, K.; Awaga, K.; Akutagawa, T.; Hasegawa, T.; Nakamura, T.; Kakiuchi, T.; Sawa, H.; Yamamoto, T.; et al. β''-(ET)$_3$(MnCl$_4$)(1,1,2-C$_2$H$_3$Cl$_3$) (ET = bis(ethylenedithio)tetrathiafulvalene); a pressure-sensitive new molecular conductor with localized spins. *J. Mater. Chem.* **2001**, *11*, 2221–2227. [CrossRef]

71. Naito, T.; Inabe, T. Structural, Electrical, and Magnetic Properties of alpha-(ET)$_7$[MnCl$_4$]$_2$·(1,1,2-C$_2$H$_3$Cl$_3$)$_2$ (ET = Bis(ethylenedithio)tetrathiafulvalene). *Bull. Chem. Soc. Jpn.* **2004**, *77*, 1987–1995. [CrossRef]

72. Willett, R.D.; Gómez-García, C.J.; Twamley, B.; Gómez-Coca, S.; Ruiz, E. Exchange coupling mediated by N–H···Cl hydrogen bonds: Experimental and theoretical study of the frustrated magnetic system in bis(o-phenylenediamine)nickel(II) chloride. *Inorg. Chem.* **2012**, *51*, 5487–5493. [CrossRef] [PubMed]

73. Palmer, W.G. *Experimental Inorganic Chemistry*; Cambridge University Press: Cambridge, UK, 1954.

74. Bain, G.A.; Berry, J.F. Diamagnetic corrections and Pascal's constants. *J. Chem. Educ.* **2008**, *85*, 532–536. [CrossRef]

75. Altomare, A.; Burla, M.C.; Camalli, M.; Cascarano, G.L.; Giacovazzo, C.; Guagliardi, A.; Moliterni, A.G.G.; Polidori, G.; Spagna, R. SIR97: A new tool for crystal structure determination and refinement. *J. Appl. Cryst.* **1999**, *32*, 115–119. [CrossRef]

76. Sheldrick, G.M. Crystal structure refinement with SHELXL. *Acta Cryst. C* **2015**, *71*, 3–8. [CrossRef] [PubMed]

77. Farrugia, L.J. WinGX and ORTEP for Windows: An update. *J. Appl. Cryst.* **2012**, *45*, 849–854. [CrossRef]